Rock and Soil Mechanics

Volume 43 | Issue 2 Article 2

4-14-2022

Physical and mechanical performance of quicklime-activated GGBS stabilized Hong Kong marine sediment at high water content

Guang-hua CAI
State Key Laboratory of Geomechanics and Geotechnical Engineering, Institute of Rock and Soil Mechanics, Chinese Academy of Sciences, Wuhan, Hubei 430071, China

Yi-fan ZHOU
Department of Civil and Environmental Engineering, The Hong Kong Polytechnic University, Kowloon, Hong Kong, China

Chi Sun POON
Department of Civil and Environmental Engineering, The Hong Kong Polytechnic University, Kowloon, Hong Kong, China

Jiang-shan LI
State Key Laboratory of Geomechanics and Geotechnical Engineering, Institute of Rock and Soil Mechanics, Chinese Academy of Sciences, Wuhan, Hubei 430071, China

Custom Citation

CAI Guang-hua, ZHOU Yi-fan, POON Chi Sun, LI Jiang-shan, . Physical and mechanical performance of quicklime-activated GGBS stabilized Hong Kong marine sediment at high water content[J]. Rock and Soil Mechanics, 2022, 43(2): 327-336.

Rock and Soil Mechanics 2022 43(2): 327–336 ISSN 1000–7598
https: //doi.org/10.16285/j.rsm.2021.5135 rocksoilmech.researchcommons.org/journal

Physical and mechanical performance of quicklime-activated GGBS stabilized Hong Kong marine sediment at high water content

CAI Guang-hua[1, 2, 3], ZHOU Yi-fan[2], POON Chi Sun[2], LI Jiang-shan[3]

1. College of Civil and Engineering, Nanjing Forestry University, Nanjing, Jiangsu 210037, China

2. Department of Civil and Environmental Engineering, The Hong Kong Polytechnic University, Kowloon, Hong Kong, China

3. State Key Laboratory of Geomechanics and Geotechnical Engineering, Institute of Rock and Soil Mechanics, Chinese Academy of Sciences, Wuhan, Hubei 430071, China

Abstract: The treatment of marine sediment has been a global-scale challenge. Portland cement (PC) is a widely-used binder in the conventional stabilization/solidification method. The use of PC can cause serious environmental pollution. In this context, the environment-friendly binder (blend of quicklime and ground granulated blast-furnace slag (GGBS)) has been adopted to replace PC in the soil remediation field. This study investigated the quicklime-activated GGBS for the stabilization of marine sediment at high water content. The physicochemical and unconfined compression tests were performed to analyze the physical, chemical, and strength characteristics of the quicklime-GGBS stabilized sediments. The results were compared with that of PC-stabilized sediment. As compared to the PC-stabilized sediment, the quicklime-GGBS stabilized sediment would generate larger volume shrinkage, lower water content, and slightly higher density. With reducing quicklime proportion and continuing curing time, the pH of the quicklime-GGBS stabilized sediment gradually decreases. The unconfined compressive strength of the lime-GGBS stabilized sediment shows a trend of first increasing (quicklime proportion of 0.05–0.15) and then decreasing (0.15–0.3) and finally increasing again (0.3–0.4). The maximum strengths appear at the lime-binder ratio of 0.15 and 0.4. The maximum strength at the quicklime-binder ratio of 0.15 is 1.4 times the same as the corresponding PC-stabilized sediment under the same condition. The findings indicate that the combination of GGBS with little quicklime has the potential to replace PC for stabilizing natural sediment at high water content.

Keywords: marine sediment; quicklime; GGBS; quicklime-binder ratio; mechanical performance

1 Introduction

Sediment dredging is a necessary regulation to maintain a sufficient depth of ports and navigation channels. About 3.89×10^6 m^3 of sediments would be annually produced during dredging in Hong Kong, China[1]. It is well-known that the soft sediments exhibit poor geotechnical properties with high compressibility and low strength due to the higher content or concentration in moisture, organic matter, salinity, and even heavy metal, which prevents the sediment from being used directly in the project[2–5]. Traditional disposal strategies for sediments include blow filling, air drying, heat treatment, and marine dumping. However, these methods usually cause lots of adverse effects such as land occupation, environmental pollution, long construction period, and huge cost[6–8]. To improve the geotechnical and environmental properties of the sediment, Portland cement (PC) is a widely-used cementitious material in the stabilization field due to its high strength gain, easy availability, and reasonable cost[9–11]. However, the production of PC consumes large amounts of energy and non-renewable raw materials. Lots of CO_2 (each ton of PC produces about 0.95 tons of CO_2, about 7% of global carbon emissions) and other deleterious gases (e.g., SO_2, CO, NO_X) are also produced during its production process[12–14]. Meanwhile, the compatibility problem between PC and soil, especially the soil containing organic matter and salinity, incurs the decay of durability unavoidably[15]. Therefore, the application of sustainable low-carbon substitutes has received increasing popularity and strong research attention in the treatment of sediment[7, 16–18].

In the past few years, extensive research has been conducted on the feasibility of the stabilizers involving industrial wastes and geopolymers composed of industrial wastes (e.g., GGBS)[7, 9, 19]. It was reported that GGBS as an iron/steel industry by-product is confirmed as the most effective substitute for PC. The GGBS has less energy consumption, lower CO_2 emissions, and lower price (60%–80% of PC) during its manufacturing process[12, 20–21]. GGBS also shows superior performance in application, such as high strength, low creep, and good durability through spontaneous hydration and time-dependent pozzolanic reactions[22]. Given this, extensive studies have been conducted to replace PC with GGBS in soil stabilization partially. It should be activated by an alkaline medium to expedite its early hydration due to the latent cementitious reactivity of GGBS[8, 12, 23–28]. Various alkaline agents are served as

Received: 18 August 2021 Revised: 4 November 2021
This work was supported by the National Natural Science Foundation of China/Hong Kong Research Grants Council Joint Research Scheme (No. N_PolyU511/18), the National Natural Science Foundation of China (No. 41902286, No. 51861165104) and the Open Fund for State Key Laboratory of Geotechnical Mechanics and Engineering (No. Z019026).
First author: CAI Guang-hua, male, born in 1985, PhD, Associate Professor, Master supervisor, research interests: environmental geotechnical engineering, solid waste recycling. E-mail: ghcai@njfu.edu.cn
Corresponding author: POON Chi-sun, male, born in 1987, PhD, PhD supervisor, research interests: environmental geotechnical engineering, solid waste recycling. E-mail: cecspoon@polyu.edu.hk

activators of GGBS, such as PC, lime, reactive MgO, calcium hydroxide, NaOH, Na_2CO_3, Na_2SO_4, and Na_2SiO_3[29–30]. In the alkali-GGBS system, the effective activation can accelerate the hydration rate of GGBS under a pH higher than 11.5[23]. According to Alibaba Mall, the prices of Na_2SiO_3 (about US$500/t), NaOH (about US$590/t), and reactive MgO (>US$500/t) are far more expensive than those of hydrated lime (about US$90/t) and quicklime (about US$60/t). When lime was used to activate GGBS, the main aim was to suppress or reduce the expansion of the sulfate-bearing soils[20, 29, 31]. In recent years, the lime-GGBS binder has been used for the production of unfired clay bricks and ground improvement, exhibiting promising superiority in durability, energy usage, and environmental benefits[32–34].

Furthermore, previous research also studied the application of the lime-GGBS binder in the stabilization of clay masonry[33], kaolinite clay, and low Oxford clay[34], the model soils of silty sand and clayey silt[35], as well as marine clay[31]. Their water contents were in a relatively low and moderate range, which was beneficial to the soil compactness and strength gain. However, there is little literature on stabilizing marine sediment at high water content using the lime-GGBS binder, and the lime-GGBS proportion governing the mechanical properties has not been determined yet. Therefore, this work attempted to use the lime-GGBS binder to stabilize marine sediment through the deep dry jet mixing method. PC was also employed in the study as a comparison. The main purposes are to study the impact of quicklime proportion on the engineering behaviors of stabilized sediments and to analyze the unconfined compressive strength. The results would facilitate the utilization of marine sediment at high water content by using a lime-GGBS binder.

2 Materials and methods

2.1 Materials

The marine sediment was obtained from Lamma Island in Hong Kong, China. The sediment transported to the laboratory was first homogenized to maintain uniformity after removing the debris and then stored in a bucket to prevent moisture loss (Fig.1(a)). The physicochemical properties of marine sediment are listed in Table 1. The initial moisture content of sediment was determined as 103.3% by drying in the oven at 105℃ for 24 h. The Atterberg limits were tested by the fall cone method, and the sediment was classified as high plasticity clay based on ASTM D2487-17e1[36]. The specific gravity of sediment was measured as 2.64 according to ASTM D854-14[37]. The particle-size distribution was tested using a laser diffraction analyzer, showing that the sediment was composed of 4.1% clay, 85.5% silt, and 10.4% sand. The pH (sediment: water = 1:2) was tested by a portable pH meter following the guidelines presented in ASTM D4972-19[38].

Table 1 Physicochemical properties of marine sediment

Classification	Index value
Natural moisture content, w_n (%)	103.3
Specific gravity, G_s	2.64
Atterberg limits	
Liquid limit, w_L (%)	62.4
Plastic limit, w_P (%)	33.5
Plasticity index	28.9
Grain-size distribution (%)[a]	
Clay (<2 μm)	4.1
Silt (2–75 μm)	85.5
Sand (>75 μm)	10.4
Mean grain size, D_{50} (μm)	10.96
Uniformity	4.08
Loss on ignition (*LOI*) [b]	11.45
pH (water/soil = 2) [c]	7.71

[a] Measured by a laser particle-size analyzer. [b] Measured by oven drying at 950°C. [c] Measured as per ASTM D4972-19[38].

The binders in this study included quicklime, GGBS, and PC used for comparison (Figs. 1b–1d). The quicklime powder (98% of CaO) from Panda Tech. Cap. Ltd. The GGBS powder was commercially available in a local grinding plant. The PC (CEM I 32.5) was produced by the Green Island Cement (Holdings) Limited. The specific surface area was measured using a nitrogen physisorption analyzer (Micromeritics ASAP2020 PLUS) per the Brunauer- Emmett-Teller (BET) method. When the specific gravity and particle-size distribution were tested, the anhydrous alcohol was used as a liquid medium to avoid any hydration of binders. The physicochemical behaviors of the three materials are given in Table 2. Fig. 2 presents morphologies of the gold-coated binders (i.e., quicklime, GGBS, and PC) revealed by a scanning electron microscope (SEM, Tecan VEGA 3), all showing similar irregular-shaped particles. Additionally, the chemical compositions of all materials obtained by an X-ray fluorescence spectrometer (XRF) are shown in Table 3. The major oxides of sediment were SiO_2 (55.6%) and Al_2O_3 (23.4%), while GGBS contained 34.2% CaO, 33.5% SiO_2, 16.4% Al_2O_3, and 11.2% MgO.

(a) Sediment (b) Quicklime

(c) GGBS (d) PC

Fig. 1 An overview of materials adopted in this study

Table 2 Physicochemical properties of quicklime, GGBS, and PC

Properties	Index value		
	Quicklime	GGBS	PC
Specific gravity, G_s	2.75	2.84	3.11
SSA (m^2/g) [a]	3.627	1.545	1.621
Mean pore diameter (nm) [a]	20.06	17.37	12.81
Grain-size distribution (%)[b]			
< 2 μm	3.0	14.8	6.0
2–75 μm	58.8	83.3	94.0
> 75μm	38.2	1.9	0.0
Average size, D_{50} (μm)	43.30	11.83	16.55
Uniformity	1.78	1.50	0.74
Loss of ignition (*LOI*) [c]	9.281	0.085	2.772
pH (water:solid = 2:1) [d]	13.84	10.77	--

Note: [a] SSA: specific surface area; [b] Measured by a laser particle-size analyzer; [c] Measured by oven drying at 950°C; [d] Based on ASTM D4972-19.

Table 3 Main components of sediment, quicklime, GGBS, and PC

Chemical composition	Sediment /%	Quicklime /%	GGBS /%	PC /%
CaO	3.030	94.000	34.200	62.000
MgO	2.930	2.620	11.200	5.900
Al_2O_3	23.400	0.710	16.400	5.530
SiO_2	55.600	1.590	33.500	18.300
Fe_2O_3	6.080	0.137	0.350	2.690
Na_2O	2.050	–	–	–
K_2O	3.210	0.091	0.595	0.690
P_2O_5	0.222	0.124	0.127	0.200
SO_3	1.170	0.671	2.110	4.310
SrO	0.021	0.041	0.065	0.110
Cl	1.280	0.006	0.030	–
TiO_2	0.782	–	0.950	0.180
MnO	0.116	–	0.328	0.040
ZnO	0.014	–	–	0.016

Note: –, not detected

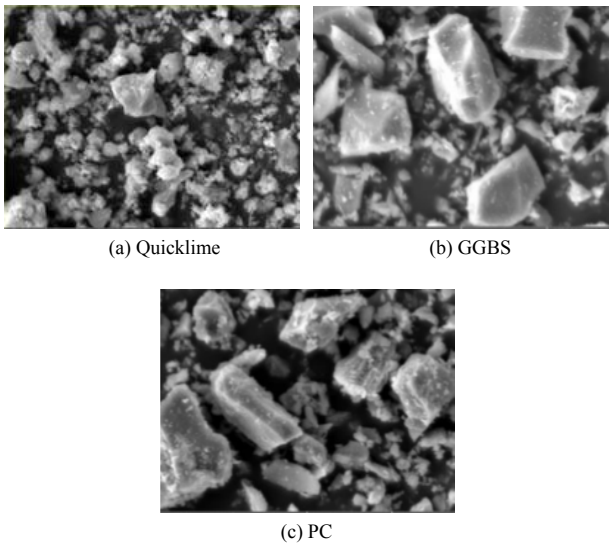

(a) Quicklime (b) GGBS

(c) PC

Fig. 2 SEM images of quicklime, GGBS, and PC at a magnification of 4.00 kx

2.2 Mixing design and specimen preparation

The amount of PC used for soil stabilization was normally ranged from 5% to 30%, as reported in the previous literature[39], and the stabilization effect of alkali-activated GGBS stabilized clay was greatly affected by the activator ratio and GGBS content (dry weight basis)[27, 29–31]. Hence, with the binder dosage of 20% where the binder dosage was the rate of the powder materials to wet sediment, six quicklime/binder (quicklime and GGBS) ratios of 0.05, 0.1, 0.15, 0.2, 0.3, and 0.4 were applied to analyze the impact of quicklime ratio on the stabilization efficiency of the sediment, and PC was used at the same dosage. In other words, the corresponding lime-GGBS (labeled as L*i*S*j*) weight ratios denoted as *i*:*j*, which were 1:19, 1:9, 3:17, 2:8, 3:7, and 4:6. The design of the mixing proportions is summarized in Table 4.

Table 4 Mixing proportions of binders used in the sediment

No.	Binder ratio			Binder content /%
	Quicklime	GGBS	Lime dosage	
L1S19	1	19	0.05	
L1S9	1	9	0.1	
L3S17	3	17	0.15	
L2S8	2	8	0.2	20
L3S7	3	7	0.3	
L4S6	4	6	0.4	
PC	–	–	–	

Note: L*i*S*j* is a binder of the quicklime-GGBS mixture at the weight ratio of *i*: *j*.

For the sample preparation, quicklime and GGBS were first mixed for 5 min by using a hand mixer. Afterward, the lime-GGBS blend/PC was added into the predetermined amount of marine sediment for another 5 min mixing to produce the uniform mixture. Subsequently, the fresh homogeneous mixtures were cast into the cubic plastic molds (40 mm× 40 mm× 40 mm) in three layers and then vibrated for 5 min to eliminate entrapped air and compact fresh samples. All the prepared specimens were put into a sealed box, which was then transferred to the curing room (23 ± 2℃, 95% ± 3% humidity). After 48 h, the samples with certain strength were successfully demoulded and then put back into the box for continuous curing.

2.3 Methods

The hydration between lime and GGBS was firstly studied by the isothermal calorimetry (Calmetrix I-Cal 4000) according to ASTM C1679[40]. When preparing the isothermal conduction calorimetry test, the lime and GGBS powder were pre-mixed together based on the designed ratios of 1:9 and 2:8. Then the pre-calculated water as per the water/binder ratio (*w*/*b*) of 0.5 was added into the lime-GGBS mixture, followed by another mixing by a mechanical stirrer. Finally, the container was sealed with a cap and transferred into the channels. The calorimetric logger was immediately started, and the data was recorded under the isothermal condition of 20℃ continuously for 96 h.

After attaining the 7, 14, and 28-day curing, the weight and size of the samples were firstly measured, and then the unconfined compressive strength (UCS) was tested at the loading rate of 1.0 mm/min by a universal compression instrument (Testometric CXM 500-50 KN) in light of ASTM D4219-08[41], where the strength was calculated. The average strength was reported by measuring triplicate samples of each mix at each curing age.

The moisture content of fresh mixtures and the broken samples after the UCS test was determined by

drying at 105℃ for at least 48 h. Based on the changes of weight, size, and water content under different curing periods, the variations of volume, density, and dry density were analyzed. After that, the dry samples were further ground to powder for the pH test. To achieve this, the plastic bottles (50 mL) containing 10 g sieved samples (< 2 mm) and 20 mL de-ionized water were first shaken for 1 h and then rested for another 1 h. According to ASTM D4972-19[38], the pH of the supernatant was tested by the portable meter under the constant ambient temperature (23 ± 2℃), and the average value of three measurements was used.

3 Results and analyses

3.1 Hydration kinetics of lime-GGBS pastes

Figures 3(a, b) present the hydration heat evolution and the heat release rate of lime-GGBS pastes for 96 h under 1:9 and 2:8 lime-GGBS ratios, respectively. Heat evolution data provide an insight into the hydration reactions between lime and GGBS over time, showing the hydration process of binders. It can be observed from Fig. 3(a) that the cumulative hydration heat of the 2:8 lime-GGBS paste was much higher than that of the 1:9 lime-GGBS paste, exhibiting a considerable heat development in less than 12 h. Obviously, the larger cumulative hydration heat was mainly ascribed to the higher CaO content in binders. Moreover, by comparing two curves, the quicklime with higher content produced a larger magnitude of hydration heat due to lime hydrolysis (ΔH = –64.45 kJ/mol)[42]. The cumulative heat of lime-GGBS pastes was very similar to that of lime-incinerated sewage sludge ash (ISSA) paste, but it was much higher compared to the alkaline-slag paste with NaOH and water glass[43–44]. The possible reason was that quicklime's alkalinity (or pH) was far higher than that of sodium water glass, and the pozzolanic reactivity of GGBS was also greater than that of ISSA[44–45].

As shown in Fig. 3(b), there was only one strong peak in the first minutes of the reaction for two lime-GGBS pastes, and the sharper peak rate was attained by a higher amount of lime which occurred immediately after that water was added into the dry binder. The sharpness could be attributed to the very fine particle size and large specific surface area of quicklime and GGBS (Table 2). Only one strong peak exhibited in this study was consistent with the heat flow curves of the alkaline-slag paste with NaOH (3.77g/100 g slag, i.e., 3.77 g NaOH activates 100 g slag) and Na_2SiO_3 (10 g/100 g slag, i.e., 10 g Na_2SiO_3 activates 100 g slag)[45], as well as the lime-ISSA paste[43]. However, this peak rate of hydration heat occurred much earlier in lime-GGBS and NaOH-GGBS pastes than that existed in the CaO-GGBS (lower content CaO), sodium water glass-GGBS, and lime-ISSA pastes[44–45]. Moreover, the hump before 6 h showed another hydration heat peak. The weak peak was postulated to be related to the pozzolanic reaction between the hydrated lime and GGBS.

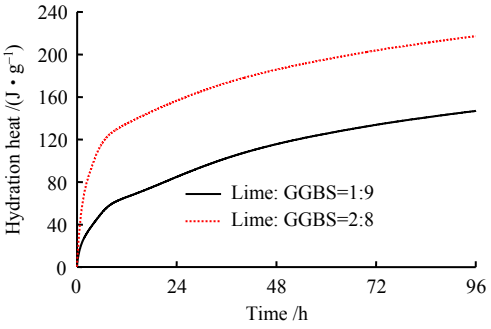

(a) Hydration heat evolution

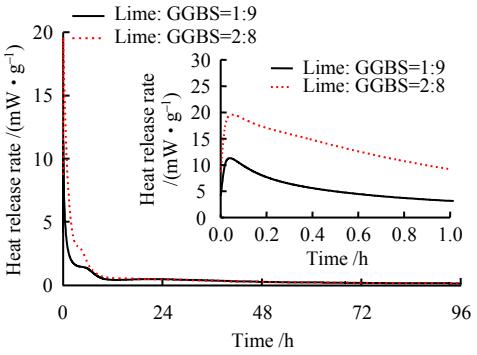

(b) Heat release rate

Fig. 3 Hydration heat of lime-GGBS pastes under two different mixing proportions (i.e., Lime: GGBS = 1:9 and 2:8) and water-binder ratio of 0.5

3.2 Physicochemical properties

3.2.1 Volume shrinkage

Figure 4 presents the volume shrinkage ratio of the lime-GGBS stabilized sediment under varying lime-binder ratios. It was evident that the volume shrinkage ratios of quicklime-GGBS stabilized sediments ranged from 6% to 10% which were significantly higher than those of PC-stabilized samples under the same curing age. The longer curing period induced larger volume shrinkage. The reason was as follows: the volume shrinkage was related to the evaporation of water during the exothermic process and air curing. Free quicklime in the lime-GGBS stabilized sediment could rapidly release much more heat in its dissolution than PC according to Zhou et al.[44] Moreover, the effective cementing component of PC was higher than that of quicklime-GGBS blend due to the total content of quicklime and GGBS being equal to the content of PC. The hydration of PC might consume more water than the hydration of GGBS to produce similar hydration products, and thus the much more free water might be lost in the lime-GGBS stabilized sediment than that in PC-stabilized sediment during the air curing. For the marine sediment with high water content (about 1.7 times of liquid limit), water was easy to evaporate under the effect of exothermic hydration of binders from the sediment mortar samples in the plastic container, leading to the volume shrinkage of specimens[46]. As shown in Fig.4, the volume shrinkage ratios of the stabilized sediment showed relatively stable values of

6%–10% when the lime-binder ratio was less than 0.3, while they quickly increased at the lime-GGBS ratio of 0.4. The results can be associated with the fact that the relatively low content of quicklime mainly promoted the hydration of GGBS, while the excessive quicklime would liberate a great amount of heat and hence the loss of moisture, causing the further volume shrinkage. To utilize the stabilized sediment as filling materials, the moderate volume shrinkage was useful for its strength gain and long-term structural stability[47]. Before the application, stable shrinkage was necessary and acceptable. In this study, the stable shrinkage ratio was 6%–10% for the quicklime-GGBS stabilized sediments.

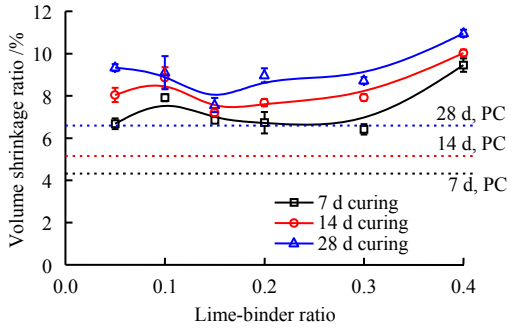

Fig. 4 Volume shrinkage ratio of lime-GGBS stabilized sediments

3.2.2 Moisture content

Figure 5 depicts the variations of the water content of the stabilized sediment with varying lime-binder ratios. It can be seen from Fig. 5 that, the water content of sediment had a significant decrease from 103% to about 70% after mixing the lime-GGBS binder. The water content slightly decreased with the increase of the lime-binder ratio, which should be ascribed to the water absorption of the binder powders and the continued consumption of water during the hydration process. When the lime-binder ratio was less than 0.2, the water content of the lime-GGBS stabilized sediment was slightly larger than that of PC-stabilized sediment. At each curing age, the moisture content of the stabilized sediment continued to decrease with increasing the lime-binder ratio, and the water content gradually decreased (Fig.5). The decrease of water content with the quicklime proportion and curing time could be attributed to the water consumption in hydration and pozzolanic reactions of GGBS and the water evaporation during the curing process.

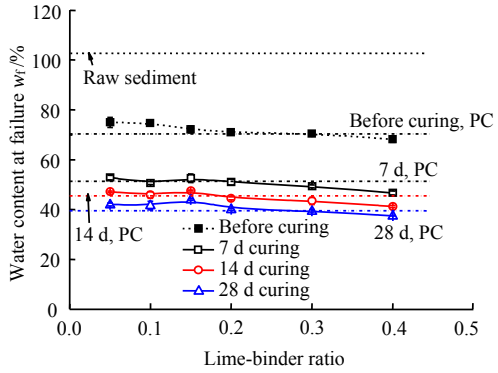

Fig. 5 Water content at the failure of lime-GGBS stabilized sediments

3.2.3 Density

According to the significant change in volume and water content as well as the slightly varied mass, the bulk density and dry density of the stabilized sediments under different conditions were calculated (Fig.6). The bulk density increased with increasing the lime-binder ratio. The bulk density of the stabilized sediment reached almost stable when the lime-binder ratio ranged from 0.1 to 0.4 except for the highest bulk density at the quicklime proportion of 0.15 (Fig.6(a)). The bulk densities of the lime-GGBS stabilized sediment were higher than those of the PC-stabilized sediment at the same curing age. Taking into account the water content, the variations in dry density of the stabilized sediment are shown in Fig.6(b). It can be observed that the dry density was relatively steady in the range of 1.0 to 1.1 g/cm^3. The dry densities of the lime-GGBS stabilized sediment were larger than those of the PC-stabilized sediment after the curing of 7 d and 14 d curing, while after 28 d curing the dry densities of two types of stabilized sediments were comparable. Moreover, it was also found that the bulk densities of all the stabilized sediments generally decreased with the curing period while the dry density significantly increased. The increase of dry density was mainly attributed to the significant reduction of volume and water content, and the growth of hydration products filling pores.

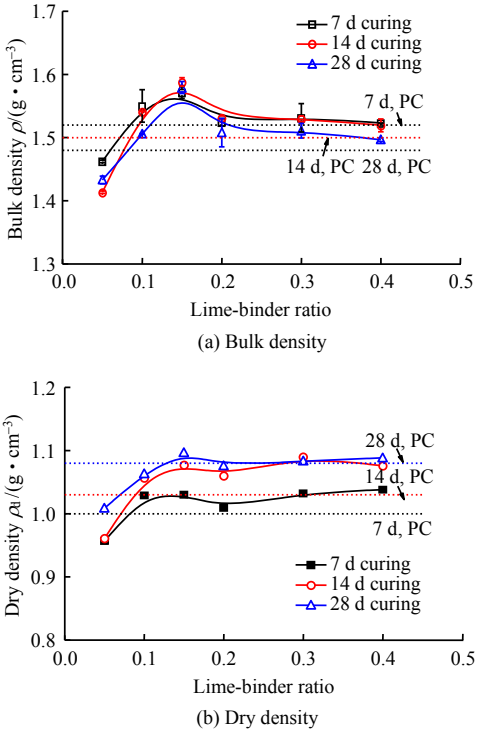

Fig. 6 The bulk density and dry density of lime-GGBS stabilized sediment

3.2.4 Soil pH

Figure 7 depicts the soil pH of the stabilized sediment with various lime-binder ratios. Although the pH of the raw sediment was 7.71 (Table 1), the pH values of the sediment stabilized by the lime-GGBS binder reached above 12.3, close to the pH of saturated $Ca(OH)_2$ solution[26]. The increased pH values of the lime-GGBS stabilized sediment were mainly attributed to the higher alkalinity of quicklime (13.84) and GGBS (10.77) (Table 2). When the lime-binder ratio was 0.1–0.15, the pH values of the stabilized sediments were almost the same as those of PC-stabilized sediments at the same curing periods. Before curing, the soil pH of the lime-GGBS-sediment mixture rapidly increased with the increase of the lime-binder ratio, and the increase rate of soil pH at the lime-binder ratio of 0.05–0.1 was larger than that of soil pH at the lime-binder ratio of 0.1–0.4. When the lime-binder ratio was 0.2, the soil pH of the binder-sediment mixture before curing was almost equal to that of the PC-sediment mixture. When the lime-binder ratio was 0.4, the pH of the binder-sediment mixture (about 13.5) was fairly close to that of pure quicklime.

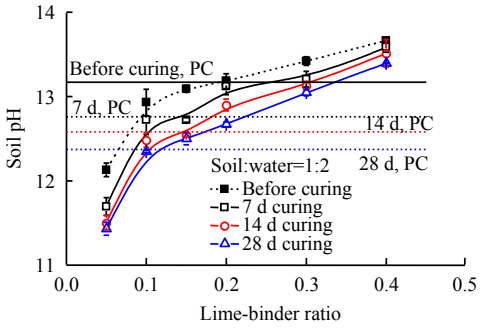

Fig. 7 Variation of pH of lime-GGBS stabilized sediments at different binder ratios

After curing of different ages, the change law for the pH value of the stabilized sediment with the lime-binder ratio was the same as that of the binder-sediment mixture, but the soil pH decreased as the curing period increased (Fig. 7). The high pH values (above 11) presented in Fig. 7 indicated that the quicklime-GGBS binder could provide a strongly alkaline environment for the hydration of GGBS. The above results could be explained by the following reasons: (ⅰ) when the lime-GGBS binder was mixed with the sediment, the hydroxyl (OH^-) released from the dissolution of quicklime (CaO) in the wet sediment, elevating the pH of pore water (refer to Eq.(1)); (ⅱ) as the lime-binder ratio increased, the soil pH increased with the dissolution of more quicklime; and (ⅲ) with the curing period, the pozzolanic reaction and the possible carbonation reaction occurred, leading to the decrease of the OH^- concentration and the corresponding pH (see Eqs.(2–5)). The pozzolanic reactions mainly took place between portlandite ($Ca(OH)_2$) and reactive SiO_2/Al_2O_3, forming the thermodynamically stable cementitious products of CSH, CAH, and CASH[48]. These reactions and hydration products would be verified in the following microanalyses.

$$CaO+H_2O\rightarrow Ca(OH)_2\leftrightarrow Ca^{2+}+2OH^- \quad (1)$$

$$Ca(OH)_2+SiO_2+H_2O\rightarrow CSH \quad (2)$$

$$Ca(OH)_2+Al_2O_3+H_2O\rightarrow CAH \quad (3)$$

$$Ca(OH)_2+SiO_2+Al_2O_3+H_2O\rightarrow CASH \quad (4)$$

$$Ca^{2+}+2OH^-+CO_2\rightarrow CaCO_3+H_2O \quad (5)$$

3.3 Unconfined compressive strength

Figure 8 shows the average strength (UCS) with a standard deviation of quicklime-GGBS stabilized sediment with varying quicklime dosage after three curing periods. For comparison, the average UCS of the PC stabilized sediment is also plotted in this figure under the same binder dosage and curing period. As shown in Fig. 8, the UCS of quicklime-GGBS stabilized sediment firstly increased and then decreased and finally caught up slightly with the increasing lime-binder ratio. The UCS of most lime-GGBS stabilized sediments was larger than the corresponding PC-stabilized sediment except for the quicklime proportion of 0.3. This might be attributed to the higher content of SiO_2 and Al_2O_3 in GGBS and thus a larger amount of CSH and CAH gel formed during GGBS hydration compared to PC (Table 3). There was an optimal lime-binder ratio (0.1-0.15) for the lime-GGBS stabilized sediment to yield the highest UCS at each curing age (i.e., 7, 14, and 28 d), and their highest UCS was much higher than the UCS of the PC-stabilized sediment at the corresponding curing time.

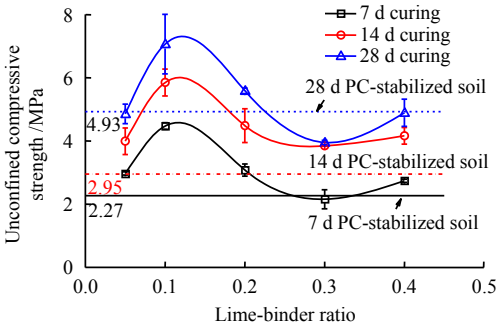

Fig. 8 Unconfined compressive strength of quicklime-GGBS stabilized sediments

Previous studies showed that other activators such as reactive MgO, carbide slag, hydrated lime, have been used in the alkali-activated GGBS stabilized soils, and the optimal proportion of activators in binders was slightly different depending on the types of soils and activators[11, 27, 30–31]. The optimal proportion (10%–20%) of activator (MgO, hydrated lime, or carbide slag) to binder yielded the highest UCS of the stabilized soils[11, 27, 31, 35]. The optimum lime-binder ratio achieving the highest UCS in this study was consistent with previous studies. However,

there was also a minimum UCS for the lime-GGBS stabilized sediment as the quicklime ratio was about 0.3. Moreover, the strength results confirmed that the increased lime-binder ratio did not always result in further growth of the strength in the lime-GGBS stabilized sediment. As the increase of lime-binder ratio caused the reduction of the GGBS content under the constant binder dosage, the decreased GGBS content led to the reduced UCS, indicating that the hydration products of GGBS should be the main contributor for the UCS development. Additionally, a slight increase in the UCS for the increasing quicklime proportion from 0.3 to 0.4 (Fig.8), could be attributed to the increasingly significant ion-exchange reaction between Ca^{2+} and mineral elements as well as the potential carbonation reaction in the sediment. The mechanism of the strength change would be further discussed through microstructure analyses.

4 Discussions

According to the above results, the water content and dry density have significant promoting effects on the strength improvement of the solidified sediments. More importantly, the significant growth in strength of the solidified sediment primarily depended on cementation products of CSH, CAH, and CASH, which were generated from the hydration reaction, ion-exchange reaction, and pozzolanic reactions under the alkali excitation, as well as the subsequent carbonation reaction (see Eqs.(2–5)). Quicklime as a good activator significantly affected the chemical reaction of GGBS. When the quicklime content was less than 10%, the strength development of the stabilized sediment was seriously hindered owing to the extremely slow hydration rate of GGBS itself. However, as the proportion of quicklime increased, the hydration rate of GGBS increased significantly. The cementing performance of GGBS needed to be activated in a sufficient alkaline environment (above 11.5). There was an optimum quicklime-binder ratio of 0.1–0.15 yielding the highest UCS which was 1.97–2.18, 1.86–1.98, and 1.41–1.44 times the UCS of PC-stabilized sediment at each curing age (7, 14, and 28 d). Besides, under such a critical lime-binder ratio of 0.1 and 0.15, the pH of the lime-GGBS stabilized sediment appeared to be close to that of PC-stabilized sediment (Fig.7), showing that the soil pH might have a certain correlation with the strength of the stabilized sediment. When pH was less than 13.25 or the quicklime content was less than 0.2, the increase of pH could facilitate the hydration of GGBS and the significant growth in strength of the stabilized sediment. However, when pH was more than 13.25, the increase of pH could restrain the strength development.

When the proportion of quicklime continued to increase from 0.3 to 0.4, the UCS had a slight increase, suggesting that the existence of enough Ca^{2+} cation was beneficial to the ion-exchange reaction and the long-term carbonation reaction. Generally, the ion-exchange capacity enhanced with the increase of ion radius (or ion valence) under the same ion concentration, and the order of cation-exchange capacity was $Na^+ < K^+ < Mg^{2+} < Ca^{2+} < Al^{3+}$ [48]. It was well known that there were plenty of Na^+ and K^+ cations on the sediment. The redundant Ca^{2+} cation from the binder was easily exchanged with the Na^+ and K^+ cations from the sediment, resulting in the reduction of double-layer thickness and thus improving the attraction of the sediment particles.

However, the quantity of each hydration product in the stabilized sediment can not be ignored, and the XRD analysis will be performed in further research. Additionally, the influence of organic matter and salt in marine sediment on the stabilization of sediment, the durability needed also to be further studied.

5 Conclusions

This work studies the solidification/ stabilization of natural sediment with high water content using a combination of lime and GGBS. A series of physical, chemical, and unconfined compression tests were performed to explain the impact of lime-binder ratios and curing period on the engineering behaviors of the stabilized sediment. main conclusions are as follows:

(1) The high lime content in lime-GGBS pastes reached the largest heat release rate in less than 1 h, and the total hydration heat of lime-GGBS paste with 2:8 over 96 h was much higher than that of the paste with 1:9 due to the presence of CaO.

(2) Compared with PC-stabilized sediment, the lime-GGBS stabilized sediment had a larger volume shrinkage ratio and similar water content. Their bulk density and dry density also showed a slight increase except for the lime-binder ratio of 0.05 and 28 day curing. Additionally, the volume shrinkage ratio and dry density of lime-GGBS stabilized sediment increased with the curing period, while the water content and bulk density decreased.

(3) With the decreased lime-binder ratio and increased curing period, the pH of the lime-GGBS stabilized sediment gradually decreased, and there seemed to be a critical lime-binder ratio of 0.1 and 0.15 where the pH of the lime-GGBS stabilized sediment was similar to that of the PC-solidified sediment. This critical pH might be the minimum pH for the hydration of GGBS.

(4) The UCS of the lime-GGBS stabilized sediment was greatly affected by the lime-binder ratio and curing period. There was an optimum lime-binder ratio ranging from 0.1 to 0.15 which yielded the highest UCS among all the mixes at each curing age.

References

[1] ZHANG Wan-lu, ZHAO Lun-yang, MCCABE BRYAN A, et al. Dredged marine sediments stabilized/solidified with cement and GGBS: factors affecting mechanical behaviour and leachability[J]. Science of the Total Environment, 2020, 733: 138551.

[2] KANG GYEONGO, TSUCHIDA TAKASHI, ATHAPATHTHU A M R G. Engineering behavior of cement-treated marine dredged clay during early and later stages of curing[J]. Engineering Geology, 2016, 209: 163–174.

[3] LANG Lei, LIU Ning, CHEN Bing. Strength development of solidified dredged sludge containing humic acid with cement, lime and nano-SiO_2[J]. Construction and Building Materials, 2020, 230: 116971.

[4] HE Jun, SHI Xiao-kang, LI Zhi-xiang, et al. Strength properties of dredged soil at high water content treated with soda residue, carbide slag, and ground granulated blast furnace slag[J]. Construction and Building Materials, 2020, 242: 118126.

[5] HO T O, TSANG D C W, CHEN W B, et al. Evaluating the environmental impact of contaminated sediment column stabilized by deep cement mixing[J]. Chemosphere, 2020, 261: 127755.

[6] ZHANG R J, DONG C Q, LU Z, et al. Strength characteristics of hydraulically dredged mud slurry treated by flocculation-solidification combined method[J]. Construction and Building Materials, 2019, 228: 116742.

[7] PU H F, MASTOI A K, CHEN X, et al. An integrated method for the rapid dewatering and solidification/ stabilization of dredged contaminated sediment with a high water content[J]. Frontiers of Environmental Science & Engineering, 2021, 15(4): 67.

[8] PU H F, KHOTEJA D, ZHOU Y, et al. Dewatering of dredged slurry by horizontal drain assisted with vacuum and flocculation[J]. Geosynthetics International, 2021. DOI: 10.1680/jgein.21.00035.

[9] PHETCHUAY C, HORPIBULSUK S, ARULRAJAH A, et al. Strength development in soft marine clay stabilized by fly ash and calcium carbide residue based geo-polymer[J]. Applied Clay Science, 2016, 127-128: 134–142.

[10] XU Bo, YI Yao-lin. Soft clay stabilization using three industry byproducts[J]. Journal of Materials in Civil Engineering, 2021, 33(5): 6021002.

[11] HO T O, CHEN W B, YIN J H, et al. Stress-strain behaviour of cement-stabilized Hong Kong marine deposits[J]. Construction and Building Materials, 2021, 274: 122103.

[12] SUMESH M, ALENGARAM U J, JUMAAT M Z, et al. Incorporation of nano-materials in cement composite and geopolymer based paste and mortar–a review[J]. Construction and Building Materials, 2017, 148: 62–84.

[13] YU Hua, YI Yao-lin, UNLUER C. Heat of hydration, bleeding, viscosity, setting of $Ca(OH)_2$-GGBS and MgO-GGBS grouts[J]. Construction and Building Materials, 2021, 270: 121839.

[14] DUNG N T, UNLUER C. Carbonated MgO concrete with improved performance: the influence of temperature and hydration agent on hydration, carbonation and strength gain[J]. Cement and Concrete Composites, 2017, 82: 152–164.

[15] PROVIS J L, PALOMO A, SHI C J. Advances in understanding alkali-activated materials[J]. Cement and Concrete Research, 2015, 78: 110–125.

[16] WANG D X, ZENTAR R, ABRIAK N E, et al. Long-term mechanical performance of marine sediments solidified with cement, lime, and fly ash[J]. Marine Georesources & Geotechnology, 2018, 36(1): 123–130.

[17] WANG Lei, CHEN Liang, TSANG D C W, et al. Recycling dredged sediment into fill materials, partition blocks, and paving blocks: technical and economic assessment[J]. Journal of Cleaner Production, 2018, 199: 69–76.

[18] HORPIBULSUK S, PHETCHUAY C, CHINKULKIJNIWAT A, et al. Strength development in silty clay stabilized with calcium carbide residue and fly ash[J]. Soils and Foundations, 2013, 53(4): 477–486.

[19] DAVIDOVITS J. Geopolymers[J]. Journal of Thermal Analysis and Calorimetry, 1991, 37(8): 1633–1656.

[20] HIGGINS D. Briefing: GGBS and sustainability[J]. Proceedings of the Institution of Civil Engineers-Construction Materials, 2007, 160(3): 99–101.

[21] YU Jia-ren, CHEN Yong-hui, CHEN Geng, et al.

Experimental study of the feasibility of using anhydrous sodium metasilicate as a geopolymer activator for soil stabilization[J]. Engineering Geology, 2020, 264: 105316.

[22] MOZUMDER R A, LASKAR A I. Prediction of unconfined compressive strength of geopolymer stabilized clayey soil using artificial neural network[J]. Computers and Geotechnics, 2015, 69: 291–300.

[23] SONG S, SOHN D, JENNINGS H M, et al. Hydration of alkali-activated ground granulated blast furnace slag[J]. Journal of Materials Science, 2000, 35(1): 249–257.

[24] YI Yao-lin, LI Cheng, LIU Song-yu. Alkali-activated ground-granulated blast furnace slag for stabilization of marine soft clay[J]. Journal of Materials in Civil Engineering, 2015, 27(4): 4014146.

[25] DU Yan-jun, WU Jian, BO Yu-lin, et al. Effects of acid rain on physical, mechanical and chemical properties of GGBS–MgO-solidified/stabilized Pb-contaminated clayey soil[J]. Acta Geotechnica, 2020, 15(4): 923–932.

[26] XU Bo, YI Yao-lin. Soft clay stabilization using ladle slag-ground granulated blastfurnace slag blend[J]. Applied Clay Science, 2019, 178: 105136.

[27] YI Yao-lin, GU Li-yang, LIU Song-yu, et al. Carbide slag–activated ground granulated blastfurnace slag for soft clay stabilization[J]. Canadian Geotechnical Journal, 2015, 52(5): 656–663.

[28] YI Yao-lin, GU Li-yang, LIU Song-yu, et al. Magnesia reactivity on activating efficacy for ground granulated blastfurnace slag for soft clay stabilisation[J]. Applied Clay Science, 2016, 126: 57–62.

[29] NIDZAM R M, KINUTHIA J M. Sustainable soil stabilisation with blastfurnace slag–a review[J]. Proceedings of the Institution of Civil Engineers-Construction Materials, 2010, 163(3): 157–165.

[30] YI Yao-lin, LISKA M, JIN Fei, et al. Mechanism of reactive magnesia – ground granulated blastfurnace slag (GGBS) soil stabilization[J]. Canadian Geotechnical Journal, 2015, 53(5): 773–782.

[31] YI Yao-lin, GU Li-yang, LIU Song-yu. Microstructural and mechanical properties of marine soft clay stabilized by lime-activated ground granulated blastfurnace slag[J]. Applied Clay Science, 2015, 103: 71–76.

[32] OTI J E, KINUTHIAJ M, BAI J. Compressive strength and microstructural analysis of unfired clay masonry bricks[J]. Engineering Geology, 2009, 109(3): 230–240.

[33] OTI J E, KINUTHIA J M, BAI J. Engineering properties of unfired clay masonry bricks[J]. Engineering Geology, 2009, 107(3): 130–139.

[34] KINUTHIA J M, OTI J E. Designed non-fired clay mixes for sustainable and low carbon use[J]. Applied Clay Science, 2012, 59-60: 131–139.

[35] YI Yao-lin, LISKA M, AL-TABBAA A. Properties of two model soils stabilized with different blends and contents of GGBS, MgO, Lime, and PC[J]. Journal of Materials in Civil Engineering, 2014, 26(2): 267–274.

[36] ASTM. D2487-17e1 Standard practice for classification of soils for engineering purposes (unified soil classification system)[S]. West Conshohocken, PA: ASTM International, 2017.

[37] ASTM. D854-14 Standard test methods for specific gravity of soil solids by water pycnometer[S]. West Conshohocken, PA: ASTM International, 2014.

[38] ASTM. D4972-19 Standard test methods for pH of soils[S]. West Conshohocken, PA: ASTM International, 2019.

[39] HORPIBULSUK S, RACHAN R, CHINKULKIJNIWAT A, et al. Analysis of strength development in cement-stabilized silty clay from microstructural considerations[J]. Construction and Building Materials, 2010, 24(10): 2011–2021.

[40] ASTM. C1679 Standard practice for measuring hydration kinetics of hydraulic cementitious mixtures using isothermal calorimetry[S]. West Conshohocken, PA: ASTM International, 2014.

[41] ASTM. D4219-08 Standard test method for unconfined compressive strength index of chemical-grouted soils[S]. West Conshohocken, PA: ASTM International, 2008.

[42] KIM M S, JUN Y, LEE C, et al. Use of CaO as an activator for producing a price- competitive non-cement structural binder using ground granulated blast furnace slag[J]. Cement and Concrete Research, 2013, 54: 208–214.

[43] ZHOU Yi-fan, LI Jiang-shan, LU Jian-xin, et al. Recycling incinerated sewage sludge ash (ISSA) as a cementitious binder by lime activation[J]. Journal of

Cleaner Production, 2020, 244: 118856.

[44] ZHOU Yi-fan, LI Jiang-shan, LU Jian-xin, et al. Sewage sludge ash: a comparative evaluation with fly ash for potential use as lime-pozzolan binders[J]. Construction and Building Materials, 2020, 242: 118160.

[45] HAHA M B, LOTHENBACH B, LE SAOUT G, et al. Influence of slag chemistry on the hydration of alkali-activated blast-furnace slag—part I: effect of MgO[J]. Cement and Concrete Research, 2011, 41(9): 955–963.

[46] LI Jiang-shan, ZHOU Yi-fan, CHEN Xin, et al. Engineering and microstructure properties of contaminated marine sediments solidified by high content of incinerated sewage sludge ash[J]. Journal of Rock Mechanics and Geotechnical Engineering, 2021, 13(3): 643–652.

[47] JIANG Ning-jun, DU Yan-jun, LIU Song-yu, et al. Multi-scale laboratory evaluation of the physical, mechanical, and microstructural properties of soft highway subgrade soil stabilized with calcium carbide residue[J]. Canadian Geotechnical Journal, 2016, 53(3): 373.

[48] LANG Lei, CHEN Bing, LI Nan. Utilization of lime/carbide slag-activated ground granulated blast-furnace slag for dredged sludge stabilization[J]. Marine Georesources & Geotechnology, 2021, 39(6): 659–669.